Numerical Investigation of the Seismic Performance of RC Columns and Entire Buildings Including Second Order Effects

Christos Zeris(✉) and Athanassios Leondaris

National Technical University of Athens, Zografou GR, 15780 Athens, Greece
zeris@central.ntua.gr

Abstract. The behaviour of reinforced concrete (RC) columns under increasing axial load and/or lateral deformation due to the seismic response of the structure, is investigated numerically considering second-order effects and their influence on the building performance. The analyses were performed with the OpenSees software, using finite elements (FE) modeling distributed damage both along the section width (fiber model) and along the column length (control sections), considering large deformations. Initially, the reliability of the modeling approach is demonstrated through verification of test results of slender column under similar loading conditions. Subsequently, the behavior of the equivalent cantilever column, which is adopted in Eurocode 2 design for large deformation effects is investigated; two alternative methods are proposed – with corresponding design nomograms being developed, for the design and capacity assessment of slender columns under seismic loading. Finally, a typical existing RC building with a tall ground floor is analyzed, both under inelastic static analysis and time integration dynamic analyses, in order to demonstrate the influence of second order deformations to the response.

Keywords: Seismic design · 2nd-order effects · Analysis · Columns · Design nomographs · OpenSees

1 Introduction and Statement of the Problem

Reinforced concrete (RC) members bearing axial loads in RC structures are subjected to 2nd-order effects due to the lateral deformations imposed in addition to initial load eccentricities due to static loads or imperfections, under lateral deformation of the structure in an earthquake. Contrary to the simplifying assumptions of initial elastic design analysis of RC structures and members, these geometrically non-linear member deformations (both global and within the member) interact with the material non-linearities of the member (cracking of the concrete, confinement, time effects and finally, yielding of the reinforcement) that define the internal and global member flexibility. The contribution of these non-linear deformations to the internal damage distribution depends both on the slenderness of the member (denoted through the slenderness ratio λ) itself and on the sway flexibility of the entire structure to which the specific member belongs. If 2nd-order effects turn out to be significant, the equilibrium of internal forces in the safety design inequality must take into account the deformed

F. Di Trapani et al. (Eds.): EOS 2022, LNCE 326, pp. 39–51, 2023.
https://doi.org/10.1007/978-3-031-30125-4_4

member geometry. In addition, 2nd-order effects will also affect the relationship between global to local deformations of the member (namely, the relationship of global – local ductility μ_θ to μ_φ) in slender members and/or sway buildings. In both cases, 2nd-order effects will lead to member and section demands considerably higher than those predicted by linear elastic design 1st-order predictions.

Experimental results on columns under increasing lateral deformation and axial compression or increasing eccentric compression ([1–6]) have shown that the bearing capacity and stiffness of the column are reduced significantly, compared to the short column. This reduction of resistance and stiffness depends on the member's slenderness ratio λ, which is expressed in terms of the member geometric characteristics: $\lambda = l_0/\sqrt{I/A}$, where l_0 is the elastic buckling length as a function of on the boundary conditions and *I, A* the moment of inertia and the cross-sectional area, respectively. For low slenderness ratios ($\lambda < 25$) the theoretical prediction for squat members applies; at medium slenderness ratios ($25 < \lambda < 80$) the column fails due to failure of the materials but at a lower load due to 2nd-order deformations, while, at high slenderness ratios ($80 < \lambda$) lateral instability with increasing strains due to P-δ takes place, followed by failure of the critical section internally.

Enforced design recommendations [7–10] correct for the equilibrium condition of the slender member due to global and internal 2nd-order deformations (P-Δ and P-δ, respectively) by applying a magnification factor of the 1st-order linear elastic moments. The greatest difficulty-uncertainty in the use of such magnification coefficients arises from the fact that it is necessary to determine, on the one hand, the sequence of actions imposed, and, on the other hand, the inelastic flexibility (1/EI effective) of the member. The member global flexibility, integrated over the entire member gradual damage distribution, gradually increases with imposed external load or deformations due to cracking and non-linearity of steel and concrete, under load and time phenomena. For this purpose, equivalent stiffnesses [11, 12] or strength reduction methods [13–16] resulting from 2nd-order effects have been proposed for the design of slender RC columns.

Eurocode 2 [7], in addition, adopts the Model Column method, based on which the behavior of the equivalent slender cantilever column is analyzed, at the critical cross-section level. Comparisons with inelastic analyses of slender cantilevers with constant initial eccentricity and increasing imposed axial load to collapse [13] showed that the moment magnification factor method is conservative at large slenderness rations and small initial eccentricities, in contrast to the Model Column method, which gave closer predictions to the failure load. Regarding the seismic loading condition, Eurocode 8 [8] specifies that 2nd-order effects (P-Δ) need not be taken into account in the building design if, in all the floors, the deformation sensitivity factor θ is limited as:

$$\theta = \frac{P_{tot} \cdot d_r}{V_{tot} \cdot h} \leq 0,10 \tag{1}$$

where: P_{tot} is the total vertical load in the seismic design situation of the floor and the floors above, d_r the design value of the inelastic relative movement of the floor, V_{tot} the floor seismic shear and h the floor height. When $0,1 < \theta < 0,2$, the seismic design load

must be increased by a factor equal to $1/(1 - \theta)$. The value of θ in Eq. (1) may not exceed the value of 0,3.

To investigate the reliability of this approach, a numerical investigation of the response of RC members and a typical existing frame were carried out, using the computer code OpenSees [18, 19], that takes into account the non-linear interaction of geometric and mechanical characteristics of RC elements. The purpose of this investigation is to contribute to a complete understanding of the phenomenon of 2nd-order effects in RC construction, leading to conservative design proposals applicable to daily design practice, based on the Eurocode 2 Model Column method [7].

2 Model Verification

2.1 Description of the Tests

In order to verify initially the reliability of the simulation with the OpenSees software [18] using the nonlinear response FE model accounting for 2nd-order effects, two experimental investigations from the literature were selected, comprising slender columns under: i) increasing eccentric axial loading intensity; or ii) constant axial load and increasing transverse loading, were initially selected and analyzed for comparison of actual and predicted response. The two tests were analyzed observing the parameters of the tests, namely loading history, member geometry and material mechanical characteristics, and the numerical and experimental response is compared herein.

2.2 Experimental Data and Numerical Prediction of the Response of Slender Column Tests

The specimens selected for FE analysis prediction had the following characteristics:

a) Column G-2 [1] with a rectangular section 4″ × 6″ (10 × 15 cm) in dimension and a ratio of height to short section dimension L/t = 20 (width in bending in the weak direction). The column section was reinforced with four 0.375″ (10 mm) diameter bars. Materials properties were as follows: 3660 psi (25.24 MPa) strength concrete and f_y = 58.8 ksi (405.4 MPa) yield strength reinforcement.

b) Two 80 mm × 80 mm rectangular cross-section columns, reinforced with four reinforcing bars of diameter 6.35mm (ρ = 1.98%), with height 1440 mm and 2400 mm (slenderness ratios of 60 and 100, respectively) [3]. Concrete had a compressive strength of 25.5 MPa and steel having a yield strength of 387 MPa was used.

The test columns were simulated in OpenSees [18] with fiber cross-sections comprising uniaxial material types *Concrete02* concrete and *Steel01* steel fibers. The members were modelled using multiple in series SEs interpolating internal curvatures (*displacement based formulation*) or a single FE interpolating internal forces (*force based formulation*) with 5 control cross sections per element in all cases, and including 2nd order phenomena under initial or subsequent large deformations [19] (*transformation corotational*). In Fig. 1, the numerical and experimental results are compared: It can be observed that, in all three slenderness ratios and loading sequences considered, the OpenSees line Fes gave the same analysis results as the experimental ones, and in

fact with different computational economy: four FEs interpolating curvatures versus were necessary to obtain the desired accuracy, compared to one FE interpolating internal forces.

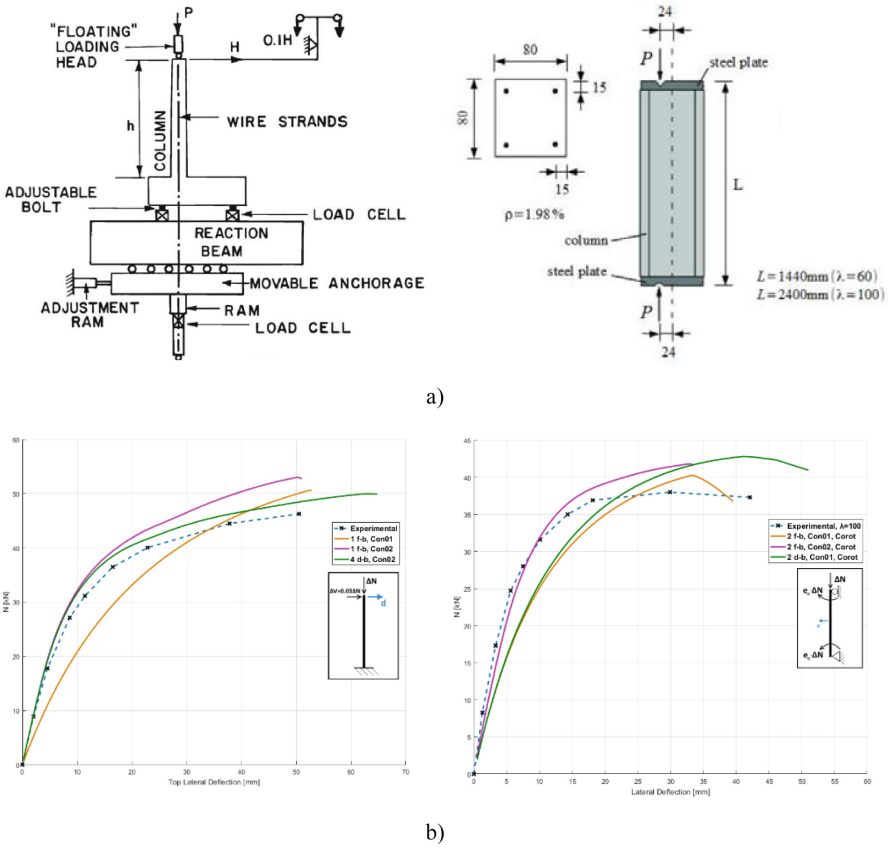

Fig. 1. a) Experimental setup and b) Comparison of numerical and test results.

3 Numerical Evaluation of the Equivalent Cantilever Column Behavior

3.1 Investigation of the Response Under Axial Loading and Transverse Deformation

Given the proven reliability of the simulation, a typical cantilever column of square cross-section was considered, under a constant axial load and a monotonically increasing lateral displacement (push-over) until failure of the critical section at the base. Slenderness ratios λ (20, 40, 60, 80, 100) were considered, with a design

normalized axial load force levels v_d between 0.20 to 0.65, namely the upper limit of Ductility Class Medium (DCM) allowed design axial force.

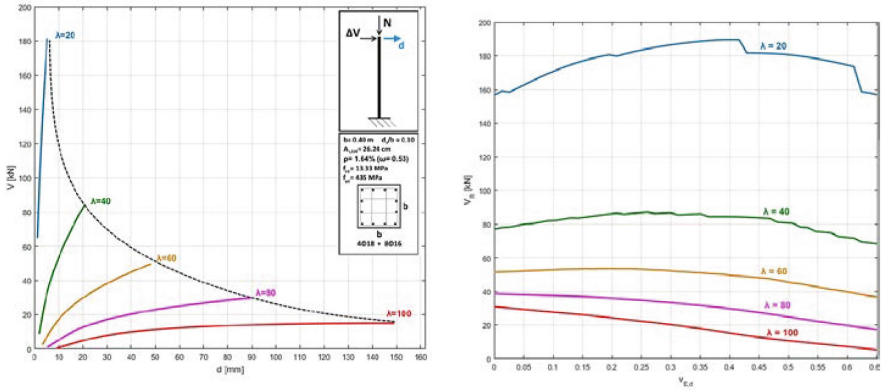

a) b)

Fig. 2. Analysis of equivalent low and medium λ cantilevers and corresponding bearing capacity under fixed axial load and lateral deformation: a) Load – tip deformation; and b) Peak resistance with imposed axial load.

All cases were analyzed considering a minimum initial construction eccentricity and no additional 1st-order static eccentricity, corresponding to the initial loading condition of a ground floor interior column between equal spans. Material models *Concrete01* (design stress-strain relations according to [7]) for unconfined concrete and *Steel01* for reinforcement [17] were adopted in the column section model. The column was modeled using a single forced-based FE with corotational transformation; following the application of the gravity initial axial force, increasing lateral deformation was imposed based on controlled deformations at the top of the cantilever, while the Newton – Raphson (N-R) algorithm was adopted for the solution.

The results of a typical analysis are shown in Fig. 2, depicting: i) the resistance – lateral deformation (*V-d*) curves for the case of a relatively low axial load level v_{Ed} = 0.40 (Fig. 2a), together with the maximum lateral resistance – axial load (V_R, v_{Ed}) curves (Fig. 2b), for all slenderness ratios. It is observed that the influence of 2nd-order effects results in a substantial reduction in both the lateral resistance and the flexural stiffness of the members for $\lambda > 20$, which, in this case, correspond with relative accuracy to the design interaction diagram of the critical section for the given geometry and material grades. Furthermore, the relationship between the imposed chord rotation ($\theta = 2d/l_o$) to the maximum curvature demand at the critical cross-section is equally influenced by increasing slenderness. One should note, further, that additional analyses [19] under simultaneously increasing axial load to the same

magnitude and lateral deformation (the case of a corner column) yielded similar peak strength demands [19] as compared to the constant axial load and increasing deformation load path above. In both cases, the computational strengths were comparable to those predicted by the Model Column method [8].

3.2 Development of Nomographs for the Design and Assessment of Slender Columns Under Seismic Loading

The inelastic response of the equivalent Model column adopted in the nominal curvature method [7] is subsequently verified numerically using the OpenSees software [17, 18], without any of the simplifications of the method regarding the internal distribution of damage. For the solution, the FE model of the previous analyses is adopted. The parametric analysis of the cantilever involves the definition of the following: i) *Geometry:* all RC columns are rectangular in cross-section with dimensions $b/h/d_1$ (namely, width, depth in the direction of bending and reinforcement location), uniformly reinforced along all four sides with a total reinforcement area $A_{s,tot}$, defined from the mechanical reinforcement ratio ω_{tot}. Namely $(A_{s,tot}/bh)(f_{yd}/f_{cd})$. ii) *Materials:* Design stress – strain characteristics were adopted for concrete (parabolic – uniform diagram) and reinforcement (elasto – plastic diagram) following [7], with corresponding design compressive strength f_{cd}, and yield strength f_{yd} respectively.

In this way, design nomograms were established, through successive analyses of a series of cantilever columns of height $l_o/2$ and slenderness λ (20 to 100, step 20), solved parametrically under increasing eccentric axial loading N_d (normalized as $v_d = N_d / bhf_{cd}$) up to failure, for a constant 1st order eccentricity e_o, equal to 0 and up to $e_o/b = 2.50$. For each nonlinear solution, the maximum bending resistance of the member at the base section M_{Rd} (normalized as $\mu_{Rd} = M_{Rd}/bh^2f_{cd}$) is projected to the initial 1st-order eccentricity $1/e_o$, yielding the peak design axial load (Fig. 3a) for the given section properties (moment reduction factor γ_{Rd} due to 2nd-order effects).

In Fig. 3c the μ_{Rd}-v_d interaction plots, derived above as a function of slenderness ratio λ, are compared with the squat column design section resistance, for the given geometry and material characteristics. Furthermore (Fig. 3d), the safety overstrength of the cantilever is established, through the evaluation of the corresponding peak axial load – bending resistance interaction using average material properties; In this way, for a given slenderness λ and an initial 1st-order eccentricity e_o (expressed as a straight line in the graph), the corresponding overstrength indices are obtained (Fig. 3e), along the eccentricity line: ratio of 2nd-order to 1st-order axial load, β_d = OA/OB – using design values, ratio of β_m = OC/OD – as before, but using average values for the material properties, and, finally, the reliabilty index of the member $\beta_{d,ov}$ = OC/OB, equal to the ratio of the bending resistance ratio based on average values with 2nd-order effects, to the 1st-order design resistance M_{Rd}.

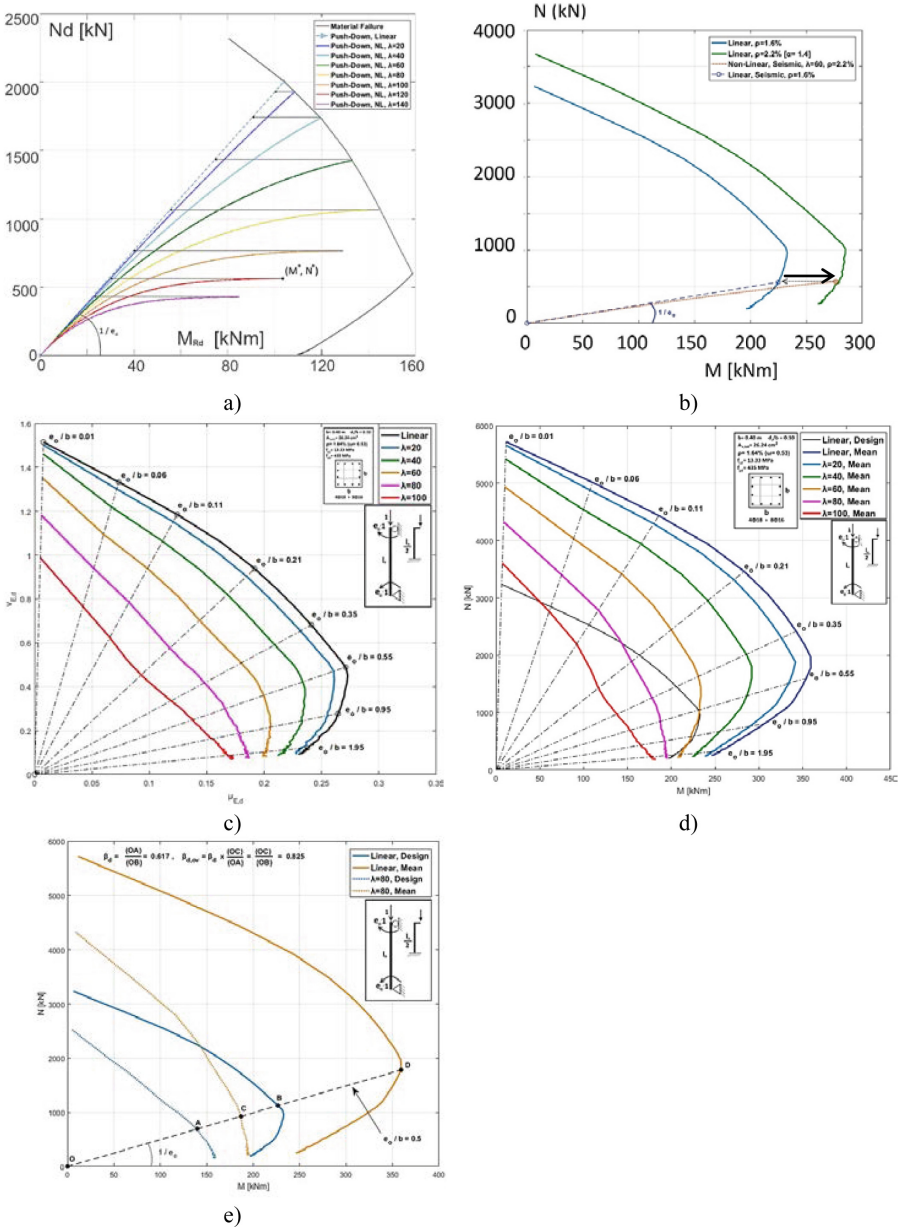

Fig. 3. Design nomographs for 2nd-order effects: a) Flexural resistance reduction due to 2nd-order effects, b) Reinforcement magnification requirement for 1st order resistance; c) Axial load – bending interaction diagrams (μ_{Ed}, v_{Ed}) versus λ, design material properties, d) Interaction diagrams using f_{cd}, f_{yd} vs f_{cm}, f_{ym}; and e) Definition of safety margins β_d, β_m and $\beta_{d,ov}$.

Using the above definitions, in Figs. 4a, b two alternative means for designing equivalent cantilever columns for 2nd-order phenomena are proposed, in the form of modified M_d - N_d interaction diagrams based on the 1st-order design demand quantities:

i) In the first case (also Fig. 3c), reduction factors of the design strength of the cantilever are established due to the 2nd-order effects, such that: $M_{Ed}{}^{I} \leq M_{Rd} / \gamma_{Rd}$, where $\gamma_{Rd} = \beta_d$. Given a 1st-order analysis, the safety inequality above is satisfied through a successive increase in the reinforcement provided, until the factored strength equals the 1st-order solution demand.

ii) In the second case (also Fig. 3b), the necessary reinforcement amplification factors are provided based on satisfying the safety inequality $M_{Ed}{}^{I} \leq M_{Rd}$. Given the 1st-order analysis, the resistance is equal to the design strength accounting for 2nd-order phenomena, while also respecting the upper limits of $\omega_{tot} < 0.04$ [7] (flat portions in Fig. 4b, where no solution is possible for given λ and e_o).

Furthermore, in terms of reliability of the column to resist the design load, by considering the shaded area in Fig. 4a, it is seen that for $\lambda > 60$ and since $\beta_{d,ov} < 1.0$, the model cantilever is unable to resist the design moment M_{Ed}, due to increased flexibility, even using average values of the material characteristics.

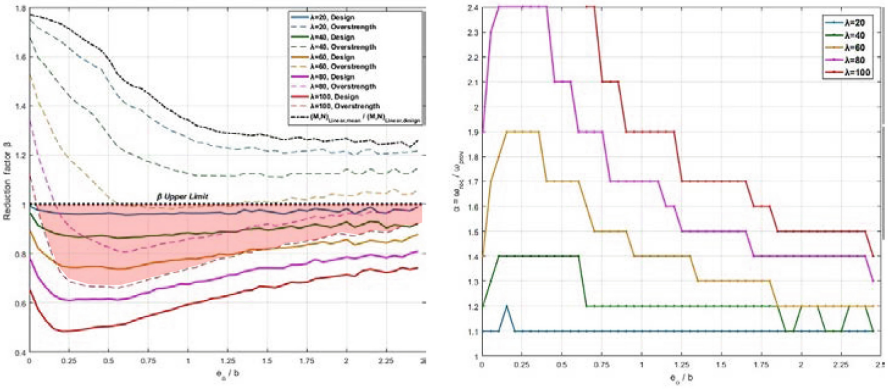

a) b)

Fig. 4. a) Design strength reduction factor β_d and b) Reinforcement amplification factor.

4 Check of an Existing Tall First Story RC Building

4.1 Building and Model Characteristics

The influence of the 2nd order effects on a typical existing five-story building with a tall first story was investigated through non-linear simulation. The building considered was five stories high, assumed to be constructed in accordance with the Regulations, geometry and materials of the 60s. The building (KB6059) was studied in earlier works [20–22] under static and time history analysis, using lumped plasticity FE models and simplified 2nd order effects based on the initial gravity loads only. The five-story RC structure had a ground floor height of 5m, typical floor heights of 3m in elevation and a

regular distribution of 4 × 3 spans in plan, 3.5 m wide each. The frame was designed for self weight and permanent loads of 1.5 kN/m^2 and a live load of 2.00 kN/m^2 for residential use. The building was assumed to be located in seismicity zone I, with an service stress seismic base shear coefficient ε = 0.04.

Internally distributed light partitions were considered as an additional uniformly distributed permanent load of 1.0 kN/m^2, while the slabs were 12 cm thick. Column cross section dimensions were 40/40 cm^2 at the ground floor, 30/30 cm^2 at the first floor and 25/25 cm^2 up to the top floor. All beams had cross section dimensions 20/50 cm^2. The formwork plan of the typical floor is depicted in Fig. 5 [20].

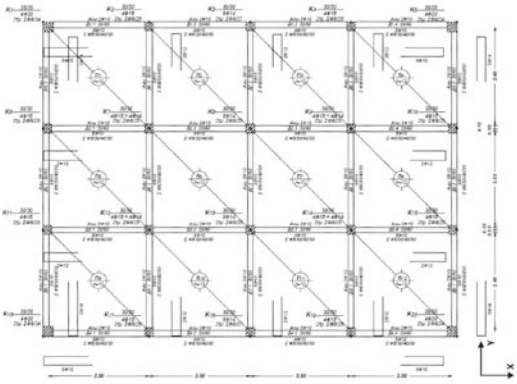

Fig. 5. Building KB6059 typical floor framing plan.

Only the intermediate bare frame was considered in the static and dynamic inelastic analyses herein; floor loads under the loading combination for the quasi-permanent loads $G_k + 0.3Q_k$ were distributed from the slabs to the longitudinal beams and the corresponding columns.

For the assessment of the seismic response herein, average values for the material characteristics were adopted: i) Concrete (model *Concrete01*) with a maximum compressive strength of 22.5 MPa at of 0.2% strain, with a softening response to failure at 0.5%; no confinement effects were considered, due to insufficient transverse reinforcement. ii) Reinforcing steel (model *Steel01*) with a yield stress of 310 MPa and a maximum rupture stress of 420 MPa, following a simplified a bilinear stress-strain diagram. A single force-based formulation FE was used per member, with five control cross-sections. For the columns, full geometric non-linearity (*corotational transformation*) was assumed; the beams were simulated as T section beams with an effective width of 1.0 m, without 2nd-order effects (*linear transformation*).

The building was analyzed under static inelastic lateral loading of increasing intensity, under the principal mode inertia load distribution (Push-Over). Subsequently, the plane frame was also analyzed using time integration, following an initial step-by step application of the vertical loads, to account for redistribution due to cracking. Full Newton-Raphson for the Push-Over and simplified Newton-Raphson for the ground excitation time history analyses were adopted as solution algorithms. The results of the inelastic analyses are subsequently described.

4.2 Static and Dynamic Inelastic Analyses Results

4.2.1 Static Push-Over Analysis

Figure 6a depicts the base shear – roof displacement Push-Over curve of the building, obtained using the linear 1st order and the corotational FE formulations (*Linear* and

Cor models, respectively). From the comparison of the two resistance curves the adoption of 2nd-order effects, even though the design axial load was relatively small for the ground floor columns of the building in question, results in a reduced base shear resistance of the slender structure, together with an overall reduction of its global deformation ductility (namely, deformation at 85% of the peak resistance, to deformation at apparent yield). Comparing the demands in the corresponding floors (Fig. 6b) it is apparent that both models exhibit the same failure mechanism, whereby all inelastic chord rotations, expectedly, concentrate at the ground floor columns, with smaller predictions by the stiffer *Linear* model.

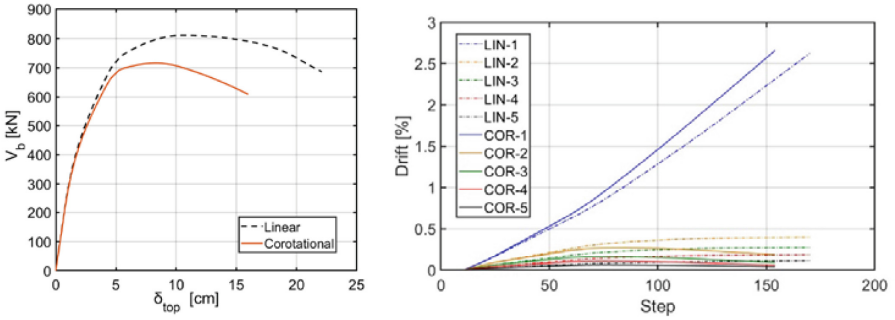

Fig. 6. Nonlinear Push-over response under increasing lateral load, *Cor* and *Linear* models: a) Comparison of load – roof deformation (P-Δ); and b) P-δ Plots of Relative Floors.

4.2.2 Time History Analyses

For the time history dynamic analysis of the of the building, the horizontal and vertical recordings of the Korinthos earthquake (1981) were considered acting simultaneously; the spectrum of the horizontal component also includes a near-field pulse ($T_p \sim 2.0$ s) affecting structures with an elastic first mode dominant period of about half of the pulse duration, such as building K60B59. As the accelerogram corresponds to a Zone with an enforced Intensity II (Peak Ground Acceleration of $\alpha_g = 0.24g$), two analyses are performed herein, as follows: i) in the first case the records are adopted with an acceleration reduction factor of 2/3 = 0.16/0.24, in order to reduce the base input to the design Zone intensity and; ii) in the second case, the actual accelerograms (factor 1.0) are used, in order to establish the response of existing RC buildings in Greece (eg, Western Athens region), designed according to seismic Zone I intensity and, after the Parnitha 1999 earthquake, are currently located in seismic Zone II.

The results of the first dynamic analysis ($\alpha_g \times 2/3$) in Fig. 7a reveal that the building responds with relatively low levels of damage under the Zone I intensity earthquake (×2/3): according to the response time history shown in Fig. 7a,b, the ground floor (as in the nonlinear static Push-Over solution) exhibits the largest relative floor deformation, equal to 1.50%, at approximately the fifth second of the seismic excitation, with little influence of the 2nd order effects, due to the relatively small axial

loads carried by the ground floor columns. On the contrary, in the case of the frame under the 1.0× excitation the solution with increased acceleration, at the same time, the failure of the ground floor columns occurred at a maximum relative floor deformation of about 3.2%. In this case, the contribution of the 2nd-order phenomena, due to the increase in lateral deformations, is significant in the dynamic response characteristics.

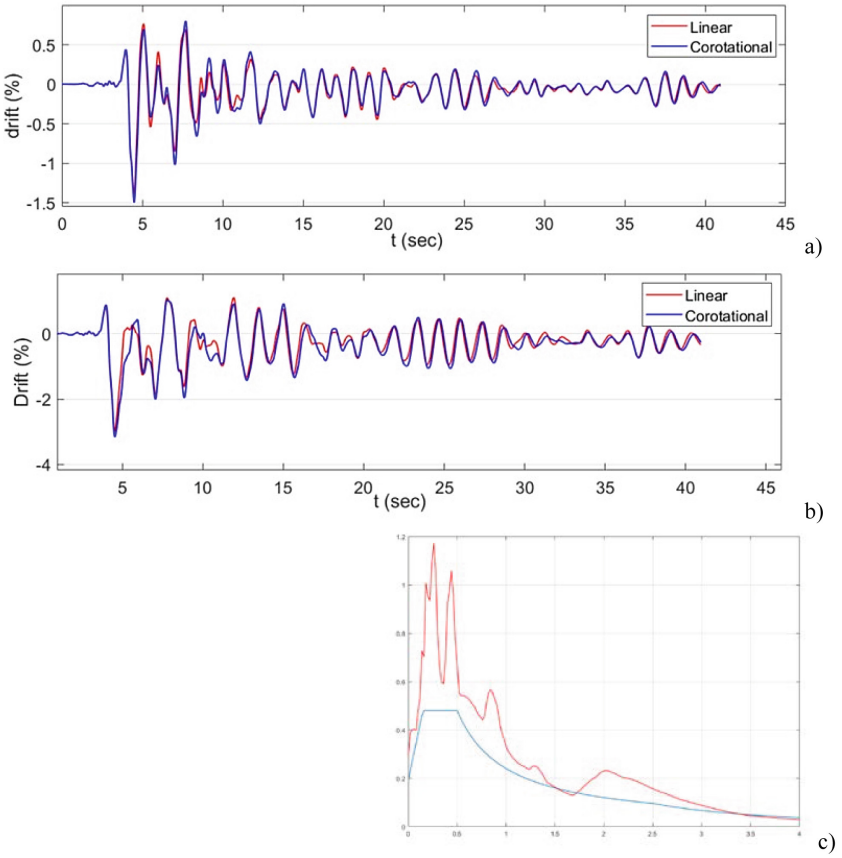

Fig. 7. a) and b) Transverse relative displacement time history of the frame ground floor, intensity x 2/3 and 1.0, respectively; and c) Pseudo-acceleration spectra (5% damping) of horizontal and vertical components of the Corinth earthquake.

5 Conclusions

Inelastic solutions of individual column elements and an entire tall 1st storey building, accounting 2nd-order column effects, have shown that columns with medium ($\lambda > 50$) to large slenderness ratios fail due to lateral instability and subsequent onset of non-linearity of the materials. Conversely, columns of moderate slenderness fail due to

material failure in the critical region, while, in areas where the slenderness ratio is less than 20, the design safety factors are sufficient. Further analysis of a typical existing building with a tall ground floor showed that the influence of the 2nd order effects was small, to the extent that the design slenderness ratios did not exceed the limiting values above. However, it is seen that design overstrength may not be sufficient for any exceedance of the design earthquake and an increase in the deformations of the building.

Using the inelastic solution and programming capabilities of the OpenSees software [18], the Model Cantilever column is analyzed and two alternative design nomographs were developed, for the 2nd-order design of columns with slenderness ratio λ and 1st-order eccentricity e_o:

- In the first case, the column ultimate strength reduction factor γ_{Rd} is obtained, due to large deformations, for use in the safety inequality with 1st-order design actions. It requires successive testing and refinement to find the ω_{tot}.
- In the second case, the magnification factor of the required percentage of reinforcement ω_{tot}, based on 1st-order design quantities, is obtained, in order to safely resist the external actions, taking into account the 2nd order effects.

References

1. Saenz, L.P., Martin, I.: Test of RC columns with high slenderness ratios. ACI J. **60**(5), 589–616 (1963)
2. Breen, J., Ferguson, P.: Long cantilever columns subject to lateral forces. ACI J. **66**(11), 884–923 (1969)
3. Breen, J.E., MacGregor, J.G., Pfrang, E.O.: Determination of effective length factors for slender concrete columns. ACI J. **69**(11), 669–672 (1972)
4. Kim, J.K., Yang, J.K.: Buckling behaviour of slender high-strength concrete columns. Eng. Struct. **17**(1), 39–51 (1995)
5. Lee, J.H., Son, H.S.: Failure and strength of high-strength concrete columns subjected to eccentric loads. ACI Struct. J. **97**(1), 75–85 (2000)
6. Mendis, P.A.: Behavior of slender high-strength concrete columns. ACI Struct. J. **97**(6), 895–901 (2000)
7. Bahn, B.Y., Tzu, C., Hsu, T.: Cyclically and biaxially loaded reinforced concrete slender columns. ACI Struct. J. **97**(3), 444–454 (2000)
8. EN1992-1-1: Eurocode 2 and NA. Design of Concrete Structures, Part 1: General Rules and Rules for Buildings. CEN, Brussels, Belgium
9. EN1998-1: Eurocode 8 and NA. Design of structures for Earthquake Resistance, Part 1: General rules, seismic actions and rules for buildings. CEN, Brussels, Belgium
10. ACI 318-19: Building Code Requirements for Structural Concrete. American Concrete Institute, Farmington Hills, Missouri, USA
11. Fib Model Code for Concrete Structures, International Federation for Structural Concrete, Lausanne, Switzerland, 402 pp. (2013)
12. Tikka, T.K., Ali, M.S.: Nonlinear EI equation for slender reinforced concrete columns. ACI Struct. J. **102**(6), 839–848 (2005)
13. Diaz, M.A., Roesset, J.M.: Evaluation of approximate slenderness procedures for nonlinear analysis of concrete frames. ACI Struct. J. **84**(2), 139–148 (1987)

14. Bazant, Z.P., Cedolin, L., Tabbara, M.R.: New method of analysis for slender columns. ACI Struct. J. **88**(4), 391–401 (1991)
15. Hellesland, J.: Nonslender column limits for braced and unbraced reinforced concrete members. ACI Struct. J. **102**(1), 12–21 (2005)
16. Kwak, H.G., Kim, J.K.: Ultimate resisting capacity of slender RC columns. Comput. Struct. **82**, 901–915 (2004)
17. Burgueño, R., Babazadeh, A., Fedak, L.K., Silva, P.F.: Second-order effects on seismic response of slender bridge columns. ACI Struct. J. **113**(4), 735–746 (2016)
18. McKenna, F., Fenves, G.L., Jeremic, B., Scott, M.H.: Open system for earthquake engineering simulation (2000). http://opensees.berkeley.edu
19. Scott, M., Filippou, F.: Response gradients for nonlinear beam-column elements under large displacements. ASCE J. Struct. Eng. **133**(2), 155–165 (2007)
20. Leondaris A. Analytical investigation of the non-linear response of slender columns and reinforced concrete buildings with second-order effects. Dissertation, Structural Design and Analysis of Constructions, School of Civil Engineering NTUA (2017). (in Greek)
21. Repapis, K., Zeris, C., Vintzeleou, E.: Evaluation of the seismic performance of existing RC buildings: II a case study for regular and vertically irregular buildings. J. Earthquake Eng. **10** (3), 429–452 (2006)
22. Zeris, C., Vintzeleou, E., Repapis, C.: Seismic performance of existing irregular RC buildings. In: Fourth European Workshop on the Seismic Behaviour of Irregular and Complex Structures, Thessaloniki (2005)